

Growth and characterization of GaAs/AlGaAs core-shell nanowires and AlGaAs nanotubes

Jinichiro Noborisaka, Junichi Motohisa, Shinjiro Hara and Takashi Fukui

Graduate School of Information Science and Technology and Research Center for Integrated Quantum Electronics, Hokkaido University, North 14 West 9, Sapporo 060-8628, Japan
nobori@rciqe.hokudai.ac.jp

ABSTRACT

We report on the growth and characterization of GaAs nanowires and GaAs/AlGaAs core-shell nanowires surrounded by {110} vertical facets on GaAs (111)B substrate. The nanowires are grown utilizing selective-area metalorganic vapor-phase epitaxy (SA-MOVPE) growth. GaAs nanowires with a typical diameter d ranging from 50 to 250 nm and a height from 2 to 9 μm were formed vertically on the substrates without any catalysts. The size of the nanowire depends on the growth conditions and the opening size of the masked substrates. After growth of GaAs nanowires, AlGaAs was grown to form free-standing heterostructured nanowires. Investigation of nanowire diameter as a function of AlGaAs growth time suggested that AlGaAs was grown on the sidewalls of GaAs nanowires, indicating that GaAs/AlGaAs core-shell structures were formed. Photoluminescence study of GaAs and GaAs/AlGaAs core-shell nanowires revealed an enhancement of PL intensity in GaAs/AlGaAs core-shell structures. Based on these core-shell nanowires, AlGaAs nanotubes were formed by using anisotropic dry etching and wet chemical preferential etching to explore new class of materials as well as to confirm the formation of core-shell structures.

Keywords: nanowires, nanotubes, GaAs, MOVPE

1 INTRODUCTION

Nanostructures such as nanotubes, nanowires, and quantum dots offer a possibility for achieving revolutionary advances towards nanotechnology-based electronics, optoelectronics, and biotechnology. *Semiconductor nanowires*, made from materials such as Si, Ge, GaP, GaAs, and InP, are new kinds of nanostructures and have been studied for their application in logic circuits¹, ultra small light emitters²⁻⁴, and nanoscale photodetectors⁵. So far, these semiconductor nanowires have been fabricated by a vapor-liquid-solid (VLS) growth method using metal catalysts⁶.

In this paper, we describe a novel approach for the formation of semiconductor nanowires and related nanostructures by using selective-area metalorganic vapor phase epitaxy (SA-MOVPE)⁷. This was inspired by the SA-

MOVPE growth of GaAs⁸ or InGaAs⁹ pillar arrays on an (111)B oriented surface for the application of photonic crystals. A similar SA-MOVPE method for InP nanowires is also reported by Pool *et al.* By using SA-MOVPE, we can fabricate nanowires at predetermined positions without the help of catalysts and we can adopt atomically precise controllability of the epitaxial growth to form heterostructures with abrupt hetero-interfaces.

2 NANOWIRE GROWTH PROCEDURE

The growth process of GaAs and GaAs/AlGaAs core-shell nanowires are schematically shown in Fig. 1. This process is essentially the same as the one for GaAs⁸, InGaAs⁹, and InP¹⁰ pillars on masked substrates except for the size of the mask opening. Firstly, after 20nm-thick SiO₂ was deposited by plasma sputtering on GaAs (111) B substrates, periodic hexagonal opening patterns were formed by electron-beam (EB) lithography, and by wet chemical etching techniques. Then SA-MOVPE of GaAs and AlGaAs was successively carried out in the opening region of the masked substrates.

For mask pattern, hexagonal openings were arranged in a triangular lattice, with the pitch a ranging from 0.4 to 3 μm . The actual shape of the opening tended to be circular because of the resolution limit in EB lithography and wet chemical etching. As we describe later, the diameter d of the nanowire is directly related to the opening diameter d_0 , and the smaller d_0 results in the longer nanowire height h .

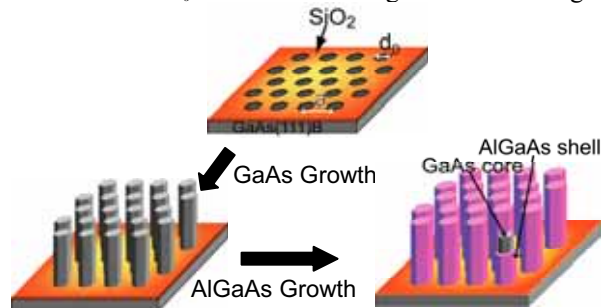


Fig1. Schematic illustration of the growth process of GaAs nanowires and GaAs/AlGaAs core-shell nanowires.

The diameter d_0 of opening area was changed from 50 to 250 nm. This periodic array of the opening pattern was only

defined in $100 \times 100 \mu\text{m}$ square regions, and outside of the square region SiO_2 was removed and the GaAs surface was exposed.

The growth was carried out in a horizontal MOVPE system working at 0.1atm. Trimethylgallium (TMG) and 20% arsine (AsH_3) diluted in H_2 were used as source materials. The partial pressure of TMG was 2.7×10^{-7} atm and that of AsH_3 was changed from 2.5×10^{-4} to 1.7×10^{-3} atm. Growth temperature was 750°C . In these conditions, the growth rate of GaAs on a planar substrate is $2.1 \text{ \AA}/\text{sec}$ for (001) and $0.3 \text{ \AA}/\text{sec}$ for (111) B, and the growth rate of the nanowires is much higher as will be discussed.

3 RESULTS AND DISCUSSIONS

3.1 Growth of GaAs nanowires

Figures 2 (a) and (b) show SEM images for two typical samples of GaAs nanowires grown on GaAs (111) B masked substrates at AsH_3 partial pressure of 5.0×10^{-4} atm. The total growth time was 20 minutes. The pattern period a is $1 \mu\text{m}$ and the diameter d_0 is 200 nm and 50 nm for the samples (a) and (b), respectively. GaAs nanowires were grown in a (111) B (vertical) direction on the substrates. As shown in the inset in Fig. 2(b), the nanowires have a hexagonal cross section. It has {110} vertical side facets similar to the larger hexagonal structure reported previously¹¹. Diameter d of the nanowires becomes smaller following to the initial opening diameter d_0 . For sample (a), the diameter d and the height h of the nanowires are 200 nm and $2.8 \mu\text{m}$, respectively, while for sample (b) these are 60 nm and $5 \mu\text{m}$, and non-uniform growth was observed. This probably originated from the non-uniform mask opening size.

Figure 3 shows the height h of GaAs nanowires versus the nanowire diameter d . The pattern period a is $0.6 \mu\text{m}$. The height h is much higher than the typical growth thickness on planar (111) B GaAs substrates (42 nm), which is indicated by the dotted line in the figure. Furthermore, h increases as d decreases. It is also noted that h also increases as $[\text{AsH}_3]$ decreases. These results are consistent with the previous results for SA-MOVPE of GaAs hexagonal structures⁸. h , however, also increases as the pitch a of the opening decreases, as shown in Fig. 3(b). We obtained the narrowest and longest nanowires with 50nm and $9 \mu\text{m}$, achieving an aspect ratio of 180 at $[\text{AsH}_3] = 2.5 \times 10^{-4}$ atm.

Within the growth conditions we used, where the growth temperature was relatively high and $[\text{AsH}_3]$ was low as compared to the ordinary GaAs growth conditions, we expected that the growth rate on (111) B would be much higher than that on (110) surfaces^{11,12}. This is because adsorbed Ga atoms cannot have strong bonding on (110) surface for small As coverage, and they can desorb very easily. In fact, according to our SEM study, almost no lateral growth over the SiO_2 mask was observed, indicating that there is almost no growth on {110} vertical surfaces

and thus $d \sim d_0$. Formation of hexagonal structures, therefore, was explained by the six-fold symmetry of the (111) B oriented surface and the fact that {110} vertical facets exhibited the slowest growth rate. The AsH_3 partial pressure dependence on the nanowire height h could qualitatively be explained by the surface reconstruction of (111) B GaAs surfaces¹³. That is, when the AsH_3 partial pressure was high, the growth of the (111) B surface was suppressed by the formation of stable As-trimers, whereas they became less stable under lower partial pressure condition, resulting in an increase in the growth rate. However, the enhancement of the growth rate on patterned substrates and the dependence of h on the pattern geometry (a and d_0) cannot be explained in a simple model.

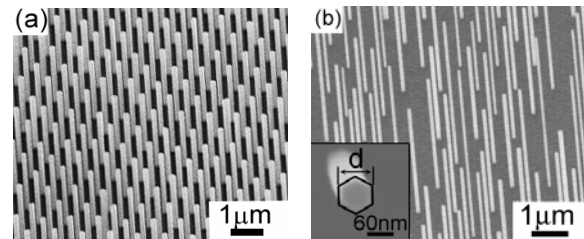


Figure. 2 (a) Bird's eyes view of thick GaAs nanowires. (b) That of thin GaAs nanowires (inset) top view.

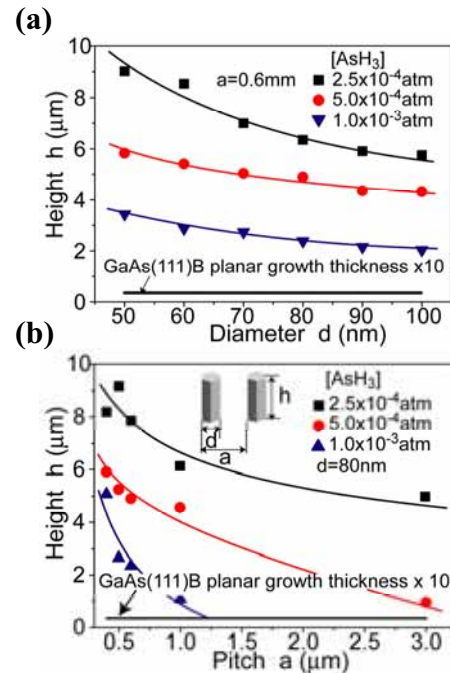


Fig. 3 (a) Dependence of nanowire height on nanowire diameter. (b) Dependence of nanowire height on pattern period.

3.2 GaAs/AlGaAs core-shell nanowires

Next, we attempted the growth of AlGaAs on the samples with GaAs nanowires. Figure 4 (a) shows a scanning electron microscope (SEM) image of nanowires

before the growth of AlGaAs. As similar to Fig. 2(a), periodic array (pitch 1micron) of free-standing GaAs nanowires was formed in the mask opening. For these nanowires, their diameters d are from 50 to 100 nm and height is 3 μm . SEM image of AlGaAs nanowires successively grown on GaAs nanowires for 10 minute is shown in Fig. 4(b). Although they maintained hexagonal shapes, we found that the nanowires became taller (5 μm) and thicker (200 ~ 300 nm). This indicates that AlGaAs were grown laterally on the sidewall of GaAs nanowires as well as on their top.

This lateral growth is confirmed by AlGaAs growth time dependence of nanowire diameter shown in Fig. 5. Here, the diameter increases as AlGaAs growth time. From these results we conclude that free-standing GaAs/AlGaAs core-shell nanowires were formed by SA-MOVPE. It follows that the thickness of AlGaAs shell was 75 to 100 nm and they are capped with 2 μm -thick AlGaAs on their top of nanowires in Fig. 4(b).

As already mentioned, these $\{110\}$ facet sidewall appears because they have slower growth rate than $(111)\text{B}$. In addition, it has confirmed that diameter d of the nanowires is directly related to the opening diameter d_0 of the mask. This means that growth on the $\{110\}$ sidewalls are negligible for GaAs grown in the present conditions. On the other hand, the growth takes place on the sidewall surfaces in the lateral direction as well as on the top surfaces for AlGaAs. Ando *et al.*¹⁴ have reported an enhanced lateral growth of AlGaAs on $\{110\}$ sidewalls of the selectively grown GaAs wire structures on $(111)\text{B}$ in slightly dissimilar conditions. The enhanced lateral growth on $\{110\}$ sidewall facet in AlGaAs could be explained by the stronger bonding on $\{110\}$ surface and lower migration length of Al atoms.

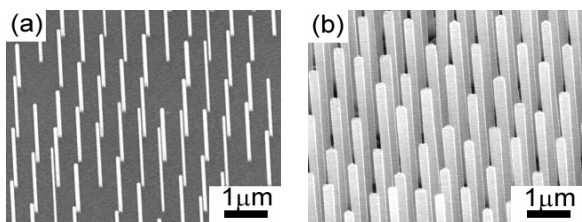


Fig. 4 (a) SEM image of GaAs nanowire before growth of AlGaAs shell. (b) That of after growth of AlGaAs shell.

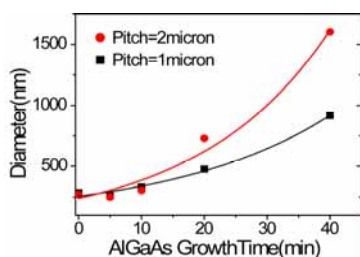


Fig. 5 Nanowire diameter as a function of the AlGaAs shell growth time.

AlGaAs lateral growth thickness as a function of the AlGaAs shell growth time is shown in Fig.5. The experiment is carried out using larger holes and longer pitches of substrate pattern to minimize the effect of size non-uniformity of core GaAs nanowires. Here, the obtained diameter of GaAs nanowires is 250 nm and their typical size fluctuation $\delta d/d$ is order of several percent⁷. We found that the amount of lateral growth of AlGaAs is non-linear and depends on the pitch a of holes. Furthermore, as we mentioned earlier, the amount of lateral growth for 10 minute growth is estimated to be 75-100nm for nanowires with $d=50\sim 80\text{nm}$, whereas it is negligible in the results of Fig.5. These mean that the lateral growth rate of AlGaAs is critically dependent on the size and arrangement of nanowires. Though it is not clear at present how the dependence of lateral growth rate is explained, the experiment suggests a presence of complicated mechanism and requires further study of accurate control of the size of core-shell heterostructures.

3.3 PL measurement

We carried out micro-photoluminescence (PL) measurement of GaAs and GaAs/AlGaAs nanowire arrays at 290K. Here, a He-Ne laser was used for excitation and the excitation intensity was 60 μW . Fig. 6 shows the PL spectra of GaAs and core-shell nanowires. The average size of nanowires is 80nm for GaAs, and 300 nm for core-shell, and pitch of the array is 0.4micron. For a reference, PL spectrum of semi-insulating (SI) GaAs substrate is also plotted. We can see some difference between two types of nanowires and the reference. Firstly, the PL intensity of core-shell nanowires is much stronger than that of bare GaAs nanowires by factor of about 20, and it is almost equals to that of SI GaAs substrate. Weak emission of GaAs nanowires is explained by nonradiative recombination of photoexcited carriers at the air-exposed GaAs sidewall surface where the high density of surface states exists. In addition, its recovery in core-shell structures is also explained by the surrounding AlGaAs barrier which prevents the coupling of photoexcited carriers in GaAs with the surface states. These results are consistent with our previous results on GaAs/AlGaAs nanowires and show a clue to obtain high-quality and optically-active nanowires.

Secondly, by comparing the PL spectra of nanowires and SI GaAs substrate, we attribute emissions at 1.45eV in nanowires is from GaAs. They both show blue-shift of 30meV from emission of GaAs bulk. In circular nanowires surrounded with infinitely high potential barriers, the ground-state quantized energy associate with lateral confinement is given by $\hbar^2 \kappa_{01}^2 / 2m d^2$, where m is the effective κ mass, d is the diameter of the nanowire and κ_{01} is the first zero of the zero-th order Bessel function: $J_0(\kappa_{01}) = 0$. If we ascribe the present blue-shift to the quantum confinement, the nanowire diameter d should

be about 20 nm, which is far smaller than the geometrical size. More detail study is required to clarify the origin of blue-shift of PL peaks in nanowires.

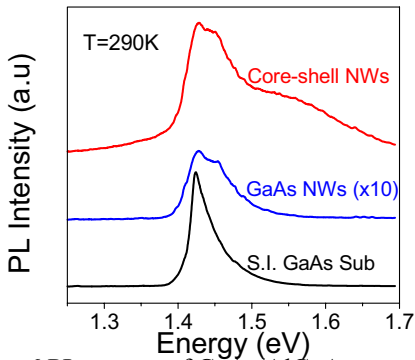


Fig. 6 PL spectra of GaAs/AlGaAs core-shell nanowires, bare GaAs nanowires and semi-insulating GaAs substrate.

3.4 AlGaAs nanotubes

Finally, we fabricated AlGaAs nanotubes out of core-shell nanowires. For this, we carried out two-step etching process, namely, anisotropic dry etching followed by preferential wet etching, on core-shell nanowires. The first etching is to selectively remove the top of GaAs/AlGaAs core-shell nanowires where 2 μm thick AlGaAs is capped, and the second is to etch selectively GaAs in the core. For dry etching, reactive ion beam etching (RIBE) using CH_4 , H_2 , Ar, and N_2 was employed for 30 min, whereas mixture of NH_4OH and H_2O_2 was used for wet etching. The result of two-step etching is shown in Fig. 7 and we obtained free-standing AlGaAs nanotubes. It is shown in the inset that the nanotubes remain hexagonal in their outer and inner part. The length of AlGaAs nanotube was 3 μm , and their inner and outer diameters were 100 nm and 200 nm, respectively. This indicates that the thickness of AlGaAs layer was 50 nm. These results are consistent with the results of SEM measurement shown Fig.4. Somewhat smaller outer diameter and tapering in nanotubes is thought to originate from side etching of AlGaAs during RIBE or from imperfect selectivity in wet etching process. Note that these nanotubes are an alternative proof for the formation of core-shell nanowires, as well as a demonstration of AlGaAs nanotubes by SA-MOVPE and simple etching processes.

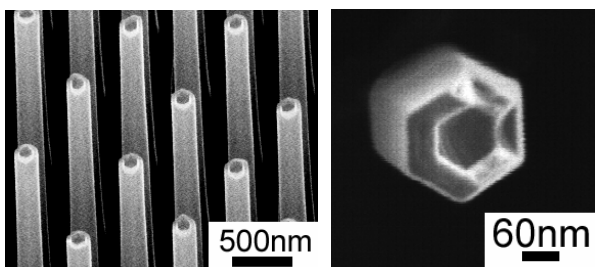


Fig. 7 SEM images of AlGaAs nanotubes.

It is also noted that our technology for fabrication of nanotube can be applied to other kind of semiconductors by an appropriate choice of dry etching gas and conditions, and solution of wet etchant. Thus, our approach is promising to explore a new class of nanoscale materials.

REFERENCES

- [1] Y. Huang, X. Duan, Y. Cui, L. J. Lauhon, K. Kim, C.M.Lieber, *Science*. **294**, 1313 (2001).
- [2] M. H. Huang, S. Mao, H. Feick, H. Yan, Y. Wu, H. Kind, E. Weber, R. Russo, P. Yang, *Science*. **292**, 1897 (2001).
- [3] N. Panev, A. I. Persson, N. Skold, and L. Samuelson, *Appl. Phys. Lett.* **83**, 2238 (2003).
- [4] X. Duan, Y. Huang, R. Agarwal, and C. M. Lieber, *Nature*. **421**, 241 (2003).
- [5] J. Wang, M. S. Gudiksen, X. Duan, Y. Cui, C. M. Lieber, *Science*. **293**, 1455 (2001).
- [6] K. Hiruma, H. Yazawa, T. Katuyama, K. Ogawa, K. Haraguchi, M. Koguchi, and H. Kakibayashi, *J. Appl. Phys.* **77**, 447 (1995).
- [7] J. Motohisa, J. Takeda, M. Inari, J. Noborisaka, T. Fukui, *Physica E*. **23**, 298 (2004).
- [8] Hamano T, Hirayama H and Aoyagi Y, *Jpn. J. Appl. Phys.* **36**, L286 (1997).
- [9] M. Akabori, J. Takeda, J. Motohisa and T. Fukui, *Nanotechnology*. **14**, 1071 (2003).
- [10] M. Inari, J. Takeda, J. Motohisa, and T. Fukui, *Physica E*. **21**, 620 (2004).
- [11] S. Ando, N. Kobayashi, H. Ando, *J. Crystal Growth*. **145**, 302 (1994).
- [12] T. Fukui, S. Ando, and Y. Tokura, *Appl. Phys. Lett.* **58**, 2018 (1991).
- [13] T. Hayakawa and M. Morishima, *Appl. Phys. Lett.* **59**, 3321 (1991).
- [14] Seigo Ando, Shi Shya Chan, Takashi Fukui, *J. Crystal Growth*. **115**, 69 (1991)